

SR 135



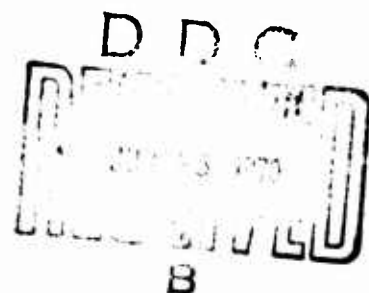
Special Report 135

AD707925

LONGITUDINAL FORCED VIBRATION OF VISCOELASTIC BARS WITH END MASS

D.M. Norris, Jr.
and
Wun-Chung Young

April 1970



RESEARCH
CLEARINGHOUSE
for Defense
Information
Requirements

GRANT NO. DA-AMC-27-021-67-G

CORPS OF ENGINEERS, U.S. ARMY
COLD REGIONS RESEARCH AND ENGINEERING LABORATORY
HANOVER, NEW HAMPSHIRE

THIS DOCUMENT HAS BEEN APPROVED FOR PUBLIC RELEASE
AND SALE; ITS DISTRIBUTION IS UNLIMITED.

32

LONGITUDINAL FORCED VIBRATION OF VISCOELASTIC BARS WITH END MASS

**D.M. Norris, Jr.
and
Wun-Chung Young**

April 1970

GRANT NO. DA-AMC-27-021-67-G21

DA TASK 1T062112A13001

CORPS OF ENGINEERS, U.S. ARMY

**COLD REGIONS RESEARCH AND ENGINEERING LABORATORY
HANOVER, NEW HAMPSHIRE**

**THIS DOCUMENT HAS BEEN APPROVED FOR PUBLIC RELEASE
AND SALE; ITS DISTRIBUTION IS UNLIMITED.**

PREFACE

This report was prepared by Dr. D.M. Norris, Jr., Associate Professor of Mechanics, of the University of New Hampshire, and Mr. Wun-Chung Young, presently Project Engineer, Combustion Engineering, Inc., Windsor, Connecticut. The work was performed for the U.S. Army Cold Regions Research and Engineering Laboratory (USA CRREL), under Grant No. DA-AMC-27-021-67-G21.

The work was under the supervision of Mr. A.F. Wuori, Chief, Applied Research Branch, and under the general direction of Mr. K.A. Linell, Chief, Experimental Engineering Division, USA CRREL. Mr. H.W. Stevens, Research Civil Engineer, of the Applied Research Branch, was the Project Leader for USA CRREL.

This report was technically reviewed by Mr. Henry W. Stevens, Mr. Ralph Lachenmaier, and Dr. Tung-Ming Lee.

The authors wish to thank Mr. Henry W. Stevens and Mr. Ralph Lachenmaier for their constructive suggestions during the course of the research.

The contents of this report are not to be used for advertising, publication, or promotional purposes. Citation of trade names does not constitute an official endorsement or approval of the use of such commercial products.

CONTENTS

	Page
Preface	ii
Nomenclature	v
Introduction	1
Theory	1
Derivation of equations for displacement, strain and stress	1
Solution in terms of the bar end acceleration ratio	3
Use of end acceleration ratio to measure the complex modulus	3
Measurement of the complex modulus at 90° phase shift	4
Stress, strain and displacement for any value of x	5
Reduction of theory to earlier work	7
Computer generated curves and discussion	7
Response curves Q versus ξ for three modes	7
Variation of ξ' with R for various values of $\tan \delta/2$	7
$\tan \delta/2$ from measured values of Q' for typical mass ratios	9
Experimental work	11
The experiment	11
Apparatus and method	11
Experimental results	14
Conclusions and summary	14
Literature cited	15
Appendix A. $\tan \delta/2$ and E^* from measured Q' and frequency	17
Appendix B. Stress, strain and displacement as a function of X and R	19
Appendix C. Q versus ξ for various R and $\tan \delta/2$ values	21
Appendix D. ξ' versus R for various values of $\tan \delta/2$	23
Abstract	25

ILLUSTRATIONS

Figure	
1. Coordinate system	2
2. Acceleration ratio Q vs frequency ratio ξ for various mass ratios R and values of damping, $\tan \delta/2$, first mode	8
3. Acceleration ratio Q vs frequency ratio ξ for various mass ratios R and values of damping, $\tan \delta/2$, second mode	8
4. Acceleration ratio Q vs frequency ratio ξ for various mass ratios R and values of damping, $\tan \delta/2$, third mode	8
5. Variation of ξ' vs mass ratio R for various values of damping, $\tan \delta/2$	8
6. $\tan \delta/2$ vs acceleration ratio Q' , first mode	9
7. $\tan \delta/2$ vs acceleration ratio Q' , second mode	10
8. $\tan \delta/2$ vs acceleration ratio Q' , third mode	10
9. Schematic of the testing system	11
10. Test specimen assembly	12
11. Experimental results, E^* vs frequency	13
12. Experimental results, $\tan \delta/2$ vs frequency	13

CONTENTS (Cont'd)**TABLES**

Table	Page
I. Stress, strain and displacement as a function of x	6
II. Computed results using experimental data	14

NOMENCLATURE

- A = Cross-sectional area of the bar
- c = Phase velocity, $c = \sqrt{\frac{E^*}{\rho}}$ sec $\delta/2$, in./sec
- C = Constant
- C_1, C_2 = Integration constants
- E = Complex modulus, psi
- E_1 = Real part of complex modulus, psi
- E_2 = Imaginary part of complex modulus, psi
- E^* = Magnitude of complex modulus, psi
- f' = Frequency of vibration when $Re = 0$, Hz
- $i = \sqrt{-1}$
- Im = Imaginary part of the ratio of the acceleration of the driven end of the bar to that of the free end
- L = Length of the test bar, in.
- m = End mass, lb-sec²/in.
- n = Mode of vibration
- $p = \frac{\omega}{c} \left(1 - i \tan \frac{\delta}{2} \right)$; see also definition below eq 4
- Q = Absolute value of the ratio of the acceleration of the free end of the bar to that of the driven end
- Q' = Measured acceleration ratio when $Re = 0$
- R = Mass ratio
- Re = Real part of the ratio of the acceleration of the driven end of the bar to that of the free end
- t = Time, sec
- u = Displacement at any section of the bar as measured on the $x - y$ coordinate system, in.
- u = Amplitude of displacement u , in.
- u_0 = Displacement at the fixed end of the bar, in.
- U_0 = Amplitude of displacement u_0 , in.
- x = Axial coordinate, in.
- y = Normal coordinate, in.

$$\gamma = \frac{m\omega^2}{pAE(i\omega)} = R\xi \left(1 - i \tan \frac{\delta}{2}\right)$$

δ = Angle by which strain lags stress, radians

ϵ = Strain, in./in.

$\bar{\epsilon}$ = Amplitude of strain in a sinusoidal excitation, in./in.

ξ = Frequency ratio, $\xi = \omega L/c$

ξ' = Frequency ratio when $\text{Re} = 0$

ρ = Mass density, lb-sec²/in.⁴

σ = Axial stress, psi

$\bar{\sigma}$ = Amplitude of stress in a sinusoidal excitation, psi

ϕ = Phase angle between bar end absolute displacements, radians

ω = Exciting angular frequency, rad/sec

ω' = Exciting angular frequency when $\text{Re} = 0$, rad/sec

LONGITUDINAL FORCED VIBRATION OF VISCOELASTIC BARS WITH END MASS

by

D.M. Norris, Jr. and Wun-Chung Young

INTRODUCTION

The U.S. Army Cold Regions Research and Engineering Laboratory (USA CRREL) employs a test technique for determining the complex moduli and damping of frozen and nonfrozen soils under vibratory loads. This involves submitting an upright cylinder of the material to vibration at the lower end with the upper end free. Input and output wave characteristics are measured by accelerometers fastened to a base plate and top plate, respectively. Other investigators are known to employ similar techniques for testing a variety of materials. In the analysis of test measurements to obtain the desired properties of the material the authors have determined the effect of the top end plate. They show that the mass of the end plate in comparison with the mass of the sample has a significant effect on the measured moduli and damping properties of the material.

A convenient method of measuring the complex modulus of a linear viscoelastic material over the audiofrequency spectrum is to apply a harmonic displacement to one end of a bar of the material and measure the ratio of end accelerations. The problem has been considered by Lee (1963) and Brown and Selway (1964) whose orientation was directed to materials as diverse as soils and polymers. The solutions given by these authors specify a free-end boundary condition. However, many experimenters using this technique have found it convenient to measure the end displacement with an accelerometer. The work presented here accounts for this end-mass effect and indicates the deviations one may expect from the simpler free-end theory.

The theoretical work presented here is supplemented by experimental results which indicate the applicability of the theory.

THEORY

Derivation of equations for displacement, strain and stress

The equation describing the motion is most easily obtained by assuming the x and y axes fixed in the bar (see Fig. 1) at the driven end $x = 0$ and the system given a displacement $u_0 = U_0 \exp(i\omega t)$.

The equation of motion is

$$\frac{\partial \sigma}{\partial x} = \rho \frac{\partial^2}{\partial t^2} (u + u_0) \quad (1)$$

2 LONGITUDINAL FORCED VIBRATION OF VISCOELASTIC BARS WITH END MASS

where σ is the uniaxial stress, ρ is the mass density and u is the axial displacement of a point in the bar measured relative to the moving coordinate system. Taking the stress at a point in the bar as $\sigma = \bar{\sigma} \exp(i\omega t)$ and the strain as $\epsilon = \bar{\epsilon} \exp[i(\omega t - \delta)]$, the constitutive law may be written as

$$\frac{\sigma}{\epsilon} = \frac{\bar{\sigma}}{\bar{\epsilon}} \exp(i\delta) \equiv E^* \exp(i\delta) \equiv E(i\omega). \quad (2)$$

Taking $u = \bar{u} \exp(i\omega t)$ and eq 2 in the form

$$\sigma = E(i\omega) \frac{\partial u}{\partial x} \quad (3)$$

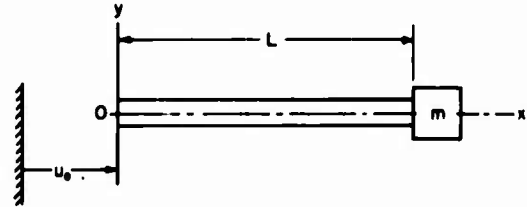


Figure 1. Coordinate system.

eq 1 goes over into the ordinary differential equation

$$\frac{d^2 \bar{u}}{dx^2} + p^2 \bar{u} = -p^2 U_0 \quad (4)$$

where $p^2 = \rho\omega^2/E(i\omega)$.

The solution to eq 4 is

$$\bar{u} + U_0 = C_1 \cos px + C_2 \sin px \quad (5)$$

where C_1 and C_2 are obtained from the boundary conditions

$$u(0, t) = 0 \quad (6)$$

$$A\sigma(L, t) = -m \frac{\partial^2}{\partial t^2} (u + u_0)_{x=L}.$$

A is the cross-sectional area of the bar and m is the end mass. Applying these boundary conditions to eq 5 the displacement solution is

$$\frac{\bar{u}(x, \omega)}{U_0} = \cos px + \left(\frac{\tan pL + \gamma}{1 - \gamma \tan pL} \right) \sin px - 1 \quad (7)$$

where

$$\gamma = \frac{m\omega^2}{pAE(i\omega)}. \quad (8)$$

The stress and strain at any point in the bar are respectively

$$\sigma = E^* \exp(i\delta) \epsilon \quad (9)$$

and

$$\epsilon = U_0 p \left[\left(\frac{\tan pL + \gamma}{1 - \gamma \tan pL} \right) \cos px - \sin px \right] \exp(i\omega t) \quad (10)$$

The solutions in eq 7-10 may be put in more meaningful form by substituting the expressions for p and γ and separating the right-hand side into real and imaginary parts. The complex result represents the magnitude of the displacement, strain or stress and the phase relative to the base displacement at any point x .

Solution in terms of the bar end acceleration ratio

A simple relationship may be found for the ratio of bar end displacements (or accelerations) that is useful in experimental measurement of the complex modulus. Rewriting eq 7 for $x = L$ gives

$$\left| \frac{u(L, \omega) + U_0}{U_0} \right| = \left| \frac{\sec pL}{1 - \gamma \tan pL} \right| = Q \quad (11)$$

It is convenient to define the frequency ratio

$$\xi = \frac{\omega L}{c} \quad (12)$$

where c is the phase velocity $\sqrt{E^*/\rho} \sec \delta/2$. Using eq 8 and 12 and the definition of p , eq 11 may be put in the form of a real and imaginary part

$$\frac{U_0}{u(L, \omega) + U_0} = \text{Re} + i \text{Im} \quad (13)$$

where it may be shown after some algebra that

$$\text{Re} = \cosh\left(\xi \tan \frac{\delta}{2}\right) (\cos \xi - R \xi \sin \xi) + R \xi \tan \frac{\delta}{2} \cos \xi \sinh\left(\xi \tan \frac{\delta}{2}\right) \quad (14)$$

and

$$\text{Im} = \sinh\left(\xi \tan \frac{\delta}{2}\right) (\sin \xi + R \xi \cos \xi) + R \xi \tan \frac{\delta}{2} \sin \xi \cosh\left(\xi \tan \frac{\delta}{2}\right) \quad (15)$$

where R is the mass ratio, $m/\rho AL$. Equations 14 and 15 are also valid for large values of δ , no simplifying assumptions having been made.

Use of end acceleration ratio to measure the complex modulus

Equations 14 and 15 suggest an experimental technique to measure the complex modulus of a linear viscoelastic material. The experimental technique for measurement of in-phase and quadrature components of the response is within the state of the art with commercially available equipment. Measurement of the complex end displacement ratio (or equivalently, the acceleration ratio) yields experimental values for Re and Im . Substitution of these two values in eq 14 and 15 yields two

4 LONGITUDINAL FORCED VIBRATION OF VISCOELASTIC BARS WITH END MASS

simultaneous transcendental equations which may be solved numerically for the two unknowns ξ and $\tan \delta/2$ for any mass ratio R . Having then solved for ξ and $\tan \delta/2$, the complex modulus may be easily obtained from eq 12 and the definition of the phase velocity c . Specifically

$$E^* = \rho c^2 \cos^2 \frac{\delta}{2} = \rho \left(\frac{\omega L}{\xi} \cos \frac{\delta}{2} \right)^2. \quad (16)$$

Hence

$$E_1 = E^* \cos \delta \quad (17)$$

and

$$E_2 = E^* \sin \delta \quad (18)$$

where E_1 and E_2 are real and imaginary parts of the complex modulus.

Measurement of the complex modulus at 90° phase shift

A simple experimental method to determine the complex modulus in the vicinity of the bar resonances was suggested by Lee (1963) and Brown and Selway (1964). The phase relationship between the end displacements is given by eq 13. If ϕ is the angle between the displacement of the driven end to the free end of the bar

$$\phi = \tan^{-1} \frac{\text{Im}}{\text{Re}}. \quad (19)$$

It follows that when $\text{Re} = 0$ there is a 90° phase shift which is easily measured experimentally without sophisticated equipment. For this case eq 14 and 15 reduce to

$$\text{Re} = \cosh \left(\xi' \tan \frac{\delta}{2} \right) (\cos \xi' - R \xi' \sin \xi') + R \xi' \tan \frac{\delta}{2} \cos \xi' \sinh \left(\xi' \tan \frac{\delta}{2} \right) = 0 \quad (20)$$

and

$$\text{Im} = \sinh \left(\xi' \tan \frac{\delta}{2} \right) (\sin \xi' + R \xi' \cos \xi') + R \xi' \tan \frac{\delta}{2} \sin \xi' \cosh \left(\xi' \tan \frac{\delta}{2} \right) = \left| \frac{1}{Q'} \right|. \quad (21)$$

Q' is the measured acceleration ratio when $\text{Re} = 0$; the frequency ratio at this point is defined as $\xi = \xi'$ and the frequency as f' .

The experimental procedure is to adjust the frequency until the phase relationship is 90°; at this point the frequency and the acceleration ratio Q' are measured. Using Q' , eq 20 and 21 may be solved numerically for ξ' and $\tan \delta/2$; hence the complex modulus may be calculated using eq 16-18. This method limits the data to a specific frequency in the vicinity of the bar's resonant frequency. ξ' does not generally coincide with ξ at resonance as is shown later in this report.

A computer program or a set of curves, both given in this report, may be used to solve for ξ' and $\tan \delta/2$ using experimental data. A computer program in Fortran IV is given in Appendix A to solve eq 20 and 21. This program uses the Newton-Raphson method (see Scarborough, 1955) to solve for ξ' and $\tan \delta/2$. The program reads R , Q' , ρ , ω' , L , mode and base amplitude and prints out

c , ξ' , $\tan \delta/2$, E^* , E_1 , E_2 and base stress. Alternatively, curves are given in the section, *Computer generated curves and discussion* (p. 7), to obtain ξ' and $\tan \delta/2$ directly using experimental values of R and Q' .

Stress, strain and displacement for any value of x

The separation of eq 7-10 into real and imaginary parts to obtain useful formulas for stress, strain and displacement as a function of x leads to complicated algebraic expressions. This effort may be circumvented by making use of the computer's ability to do complex arithmetic directly. The stress, strain and displacement were evaluated at five stations along the bar for various mass ratios. Typical results are given in Table I. The computer program is given in Appendix B. Values given are for a soil with $E^* = 78,000$ psi and $\tan \delta/2 = 0.06$.

The maximum stress occurs at $x = 0$ for the first three modes. An expression for this stress derived from eq 9 and 10 is

$$\sigma(0, \omega) = E(i\omega) U_0 p \left(\frac{\tan pL + \gamma}{1 - \gamma \tan pL} \right). \quad (22)$$

Applying the complex definitions of p , $E(i\omega)$ and γ , and considering the simple case when the 90° phase shift occurs ($\text{Re} = 0$), one has

$$\sigma(0, \omega) = \frac{U_0 \xi' E^* Q'}{L} \left[\bar{I} \tan \frac{\delta}{2} - \bar{R} - i \left(\bar{R} \tan \frac{\delta}{2} + \bar{I} \right) \right] \quad (23)$$

where

$$\bar{R} = (\cos \xi' - R \xi' \sin \xi') \sinh \left(\xi' \tan \frac{\delta}{2} \right) + R \xi' \tan \frac{\delta}{2} \cos \xi' \cosh \left(\xi' \tan \frac{\delta}{2} \right)$$

$$\bar{I} = (\sin \xi' + R \xi' \cos \xi') \cosh \left(\xi' \tan \frac{\delta}{2} \right) + R \xi' \tan \frac{\delta}{2} \sin \xi' \sinh \left(\xi' \tan \frac{\delta}{2} \right)$$

and Q' is the experimentally measured value of the acceleration ratio at a 90° phase shift. The magnitude of the stress is given by

$$|\sigma(0, \omega)| = \sqrt{\text{Re}^2(\sigma) + \text{Im}^2(\sigma)}. \quad (24)$$

This calculation is built into the standard program for calculating $\tan \delta/2$ and E^* from experimental data (see Appendix A).

Table I. Stress, strain and displacement as a function of x .
Only absolute values are shown for each variable. The phase relationship between these variables is available from the computer program printout (see Appendix B).

Mode	x	$R = 0$				$R = 0.1$				$R = 0.5$			
		$\bar{u}-\mu$ in.	$\bar{\sigma}$ -psi	$\bar{\epsilon}-\mu$ in./in.	$\bar{u}-\mu$ in.	$\bar{\sigma}$ -psi	$\bar{\epsilon}-\mu$ in./in.	$\bar{u}-\mu$ in.	$\bar{\sigma}$ -psi	$\bar{\epsilon}-\mu$ in./in.	$\bar{u}-\mu$ in.	$\bar{\sigma}$ -psi	$\bar{\epsilon}-\mu$ in./in.
$n = 1$	0.000	0	26.09	334	0	23.76	305	0	18.78	0	0	18.78	241
	0.25L	814	24.06	309	745	22.24	285	594	18.10	594	594	18.10	232
	0.50L	1503	18.40	236	1395	17.92	230	1146	16.12	1146	1146	16.12	207
	0.75L	1984	9.96	128	1879	11.35	146	1616	12.98	1616	1616	12.98	166
	1.00L	2125	0.0	0	2108	3.36	43	1969	8.91	1969	1969	8.91	114
$n = 2$	0.000	0	26.71	342	0	24.58	315	0	23.73	0	0	23.73	304
	0.25L	673	11.22	144	651	12.58	161	664	15.06	664	664	15.06	193
	0.50L	565	18.54	238	659	13.33	171	837	6.30	837	837	6.30	81
	0.75L	365	23.78	305	264	23.65	303	429	21.15	429	429	21.15	271
	1.00L	727	0.0	0	664	9.40	121	429	20.23	429	429	20.23	259
$n = 3$	0.000	0	27.91	358	0	26.11	335	0	26.35	0	0	26.35	338
	0.25L	475	13.24	170	500	9.94	127	542	7.88	542	542	7.88	101
	0.50L	402	18.67	239	343	21.89	281	307	24.59	307	307	24.59	315
	0.75L	222	23.36	300	350	15.52	199	493	5.93	493	493	5.93	76
	1.00L	454	0.0	0	397	13.84	177	240	23.22	240	240	23.22	298

Reduction of theory to earlier work

For $\tan \delta/2 = 0$ eq 14 and 15 reduce to the equation for the eigenfrequencies of an elastic bar, i.e.

$$\cot \xi = R\xi \quad (25)$$

as given by Timoshenko (1955).

For $R = 0$ (but including damping), eq 20 and 21 reduce to those given by Brown and Selway (1964), i.e.

$$\xi' = \frac{\pi}{2} (2n - 1) \quad (26)$$

and

$$\tan \frac{\delta}{2} = \frac{2 \sinh^{-1} \left(\frac{1}{Q'} \right)}{\pi(2n - 1)} \quad (27)$$

where the notation has been changed to conform to this report. The latter two equations are similar to those given by Lee (1963) if the small angle assumption is made and only the first mode is considered.

COMPUTER GENERATED CURVES AND DISCUSSION

Response curves Q versus ξ for three modes (Fig. 2-4)

Figures 2-4 give the absolute value of the acceleration ratio of the free end of the bar to the driven end (defined as Q) as a function of the frequency ratio ξ for three modes of vibration. In generating these curves, $\tan \delta/2$ was arbitrarily set at a constant value for each curve although in a real material one would expect some variation with frequency. ξ was incremented and values of Q and ξ were plotted for selected values of mass ratio R . In each mode the effect of end mass is obvious. The resonant frequency is lowered dramatically with increased R and there is also a decrease in Q_{\max} , the maximum value of the response.

The computer plotter was programmed to print a plus sign on the Q versus ξ curves (see Fig. 2-4 and Appendix C) when the phase relationship was 90° (corresponding to $\text{Re} = 0$), the convenient experimental point discussed in the section, *Measurement of the complex modulus at 90° phase shift* (p. 4). This point corresponds to specific values of ξ' and Q' also discussed previously. Unless $\tan \delta/2$ is very small, Q' does not coincide with Q_{\max} but is shifted to the higher frequency side of resonance. For the first mode with $R = 0$, eq 20 reduces to $\cos \xi' = 0$; hence ξ' is $\pi/2$ for any value of $\tan \delta/2$ as seen in Fig. 2. However, for $R > 0$ it is seen that ξ' actually increases with increased $\tan \delta/2$ for a given mass ratio R although the true resonant frequency is lowered with increased $\tan \delta/2$. Experimenters must not confuse Q_{\max} with Q' .

Variation of ξ' with R for various values of $\tan \delta/2$ (Fig. 5)

ξ' is an important quantity in the theory since it is used to compute the magnitude of the complex modulus E^* using eq 16. Figure 5 is a computer generated plot of the variation of ξ' with R for

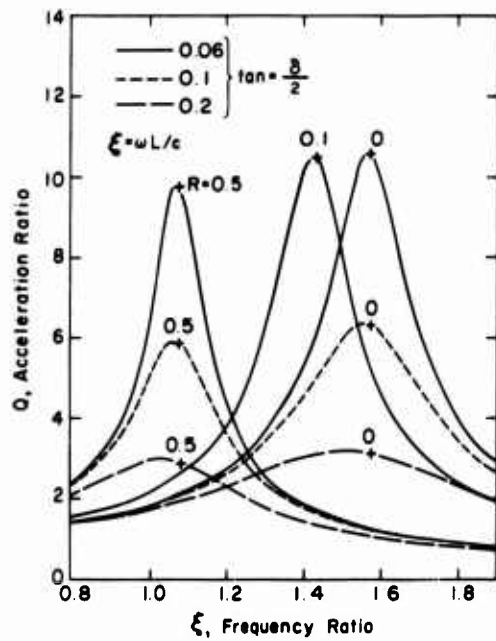


Figure 2. Acceleration ratio Q vs frequency ratio ξ for various mass ratios R and values of damping, $\tan \delta/2$, first mode.

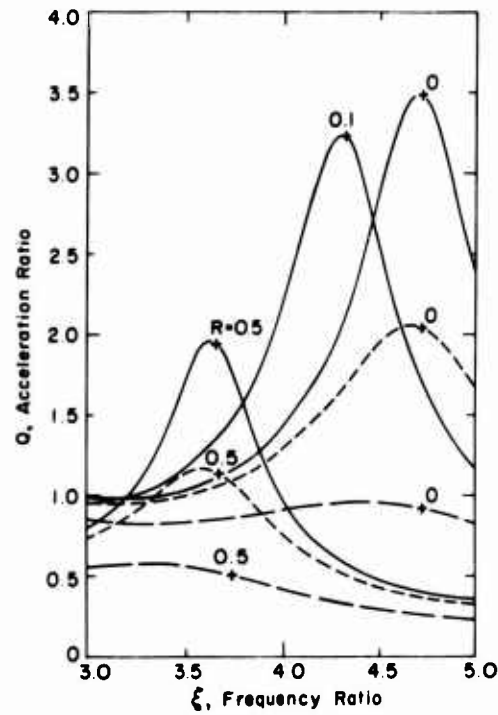


Figure 3. Acceleration ratio Q vs frequency ratio ξ for various mass ratios R and values of damping, $\tan \delta/2$, second mode.

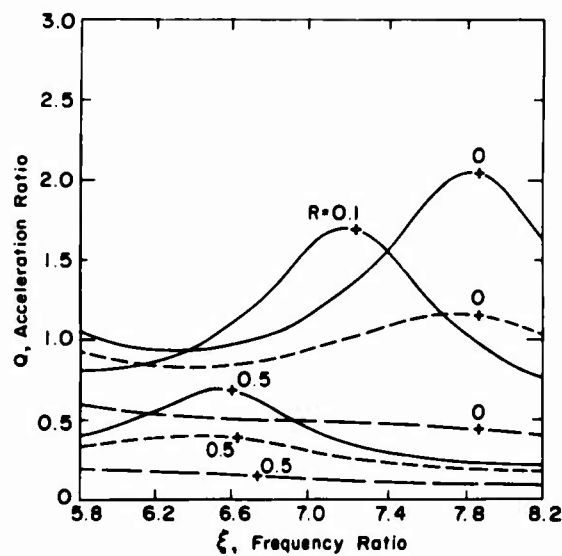


Figure 4. Acceleration ratio Q vs frequency ratio ξ for various mass ratios R and values of damping, $\tan \delta/2$, third mode.

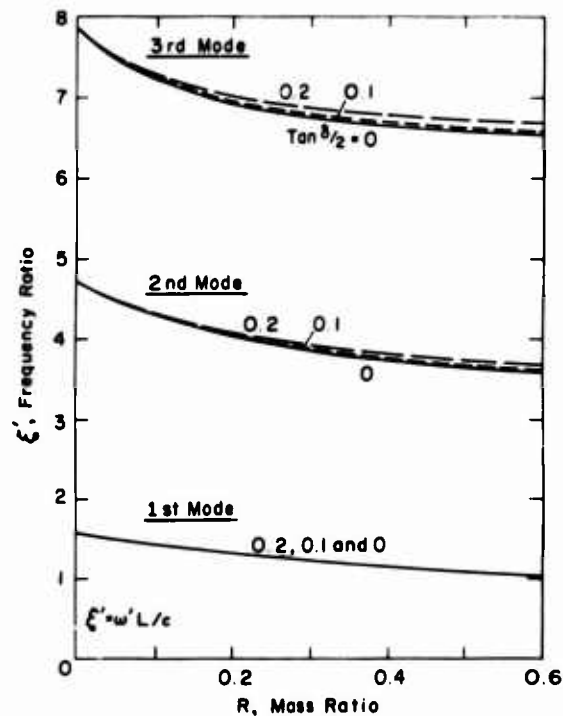


Figure 5. Variation of ξ' vs mass ratio R for various values of damping, $\tan \delta/2$.

various values of $\tan \delta/2$. ξ' decreases significantly with increased R especially for the higher modes. For any given value of R , ξ' increases with an increase of $\tan \delta/2$ as previously seen from Fig. 2. Fig. 5 was generated from eq 20; $\tan \delta/2$ was specified and for an incremented value of R a half interval search method (see Kuo, 1965) was used to find and plot the values of ξ' . The computer program is given in Appendix D.

Tan $\delta/2$ from measured values of Q' for typical mass ratios (Fig. 6-8)

These curves permit the determination of $\tan \delta/2$ from experimentally measured values of Q' for selected values of mass ratio R . The computer program of Appendix A used to solve eq 20 and 21 was used to generate these curves.

These curves plot as a straight line on log-log paper down to a certain value of Q' (about 4.0 for the first three modes) and then show a slow deviation. This implies there exists a relationship over the linear range in each mode of the form

$$Q' \tan \frac{\delta}{2} = \frac{1}{C} \quad (28)$$

where the constant C is a different number for each value of R . It is easy to show from Fig. 6 or directly from eq 20 and 21 that for $R = 0$ the constant in the first mode is $\pi/2$.

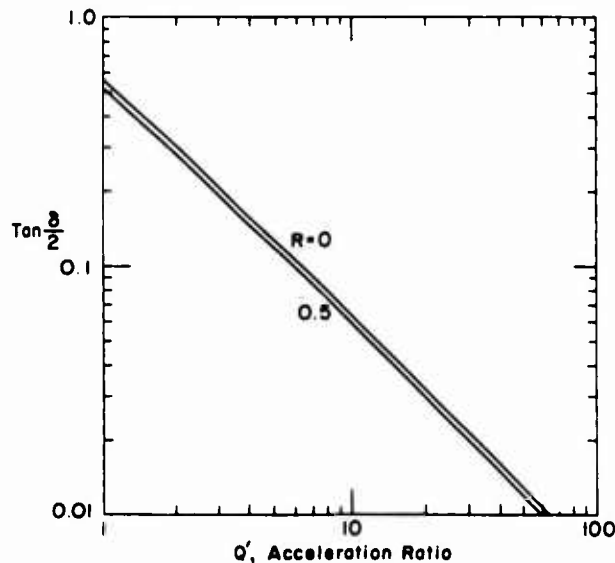


Figure 6. Tan $\delta/2$ vs acceleration ratio Q' , first mode.

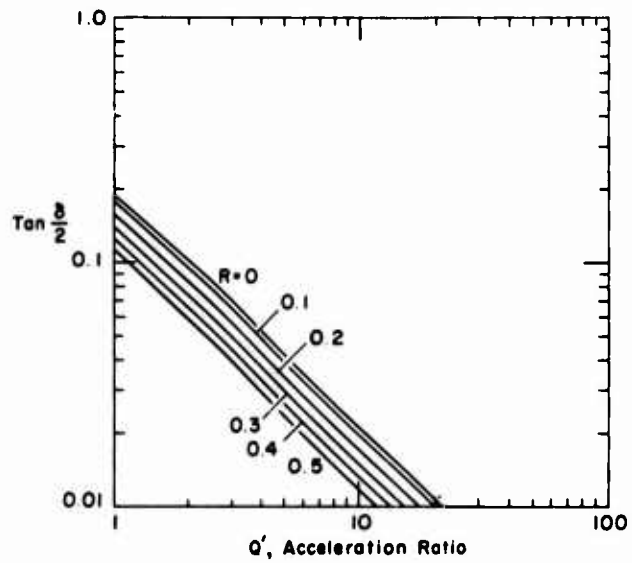


Figure 7. $\tan \delta/2$ vs acceleration ratio Q' , second mode.

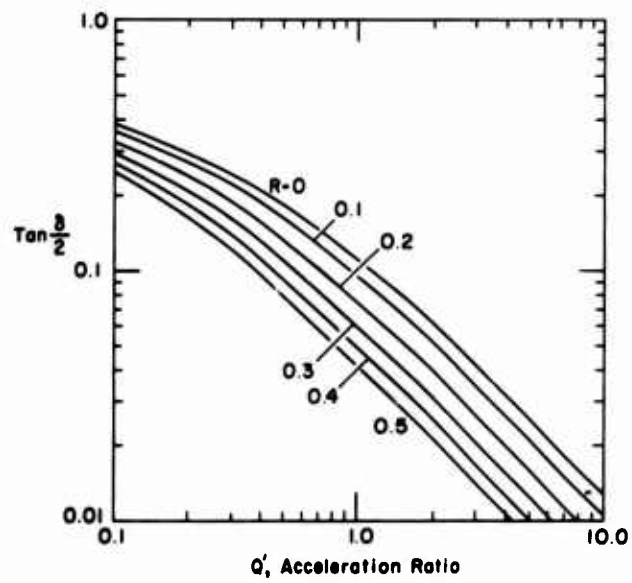


Figure 8. $\tan \delta/2$ vs acceleration ratio Q' , third mode.

EXPERIMENTAL WORK

The experiment

The objective of the experimental work was to check the applicability of eq 20 and 21, which include the mass loading effect in the measurement of the dynamic modulus. To do this the theory of the section, *Measurement of the complex modulus at 90° phase shift* (p. 4), was employed using a polymer bar to simulate a soil sample.

The experiment consisted of driving the bar with a small end mass in the first three modes and measuring Q' , the measured acceleration ratio, and f' , the frequency where the 90° phase shift occurred. The test was then repeated with a larger end mass, with the bar shortened to maintain a constant frequency in each mode. The computer program of Appendix A was then used to compute E^* and $\tan \delta/2$, both of which should be invariant with respect to mass ratio R since the assumption of the theory is that E^* and $\tan \delta/2$ are functions only of frequency and are independent of R . The check then was the coincidence of E^* (or $\tan \delta/2$) measured at various mass ratios when plotted at the constant frequency.

Apparatus and method

A schematic diagram of the testing system is shown in Figure 9. The source of sinusoidal displacement was an MB Electronics Model EA 1500 electromagnetic exciter which was driven by an amplifier and audio oscillator (signal generator). A frequency counter was used to measure frequency. Two piezoelectric accelerometers were employed to measure acceleration at the ends of

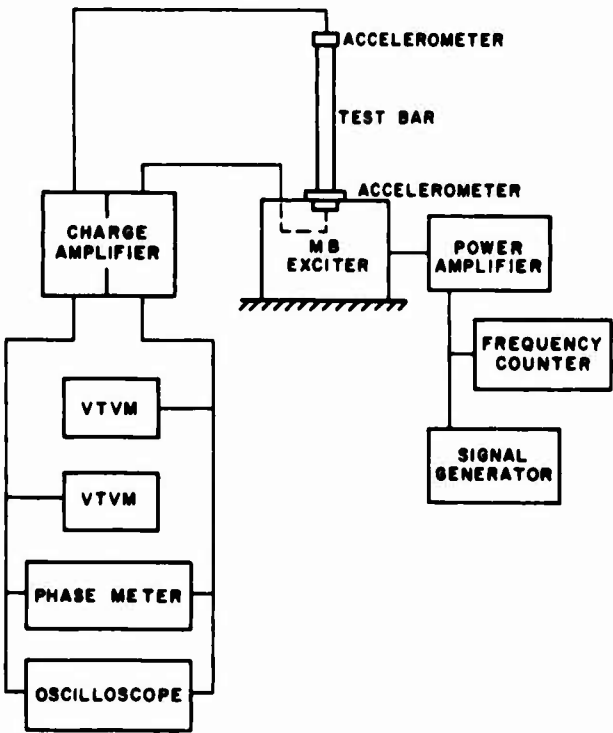


Figure 9. Schematic of the testing system.

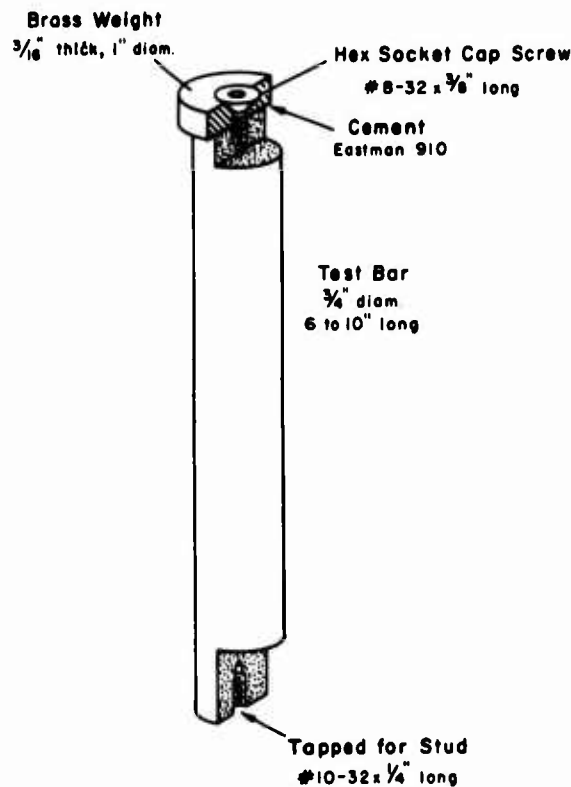


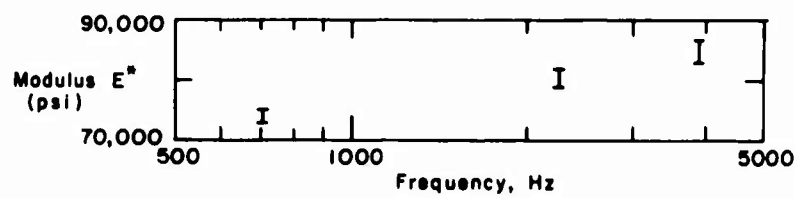
Figure 10. Test specimen assembly.

the bar. The output from the accelerometers was fed into two charge amplifiers and read from two vacuum tube voltmeters. The amplified signals were displayed on a two-channel oscilloscope and the phase shift was observed on the oscilloscope. It was found that the phase of the two signals could be accurately measured on the oscilloscope; hence in the latter part of the experiment the phasemeter employed in earlier experiments was omitted.

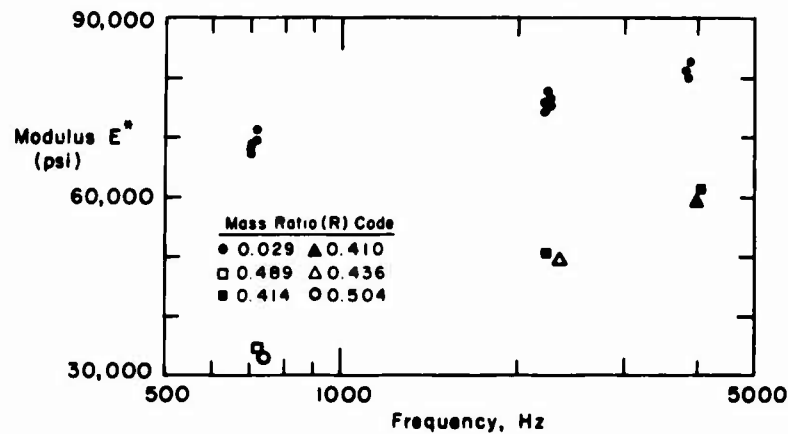
The test specimens were 3/4-in.-diam bars of low density polyethylene. The measured specific gravity of this material was 0.915. The bars were used as received from the supplier with no heat treatment and only the ends machined. All testing was done at $75^{\circ}\text{F} \pm 2^{\circ}\text{F}$. The method of fastening the end mass and fixing the bars to the exciter is shown in Figure 10. A 2-gram accelerometer was glued with Eastman 910 cement directly to the mass or in the case of the low mass tests directly to the free end of the bar. Bar lengths are given in Table II.

Calibration of the accelerometers was done at the three frequency ranges of interest (data were recorded in the first three modes) at the driving magnitude by driving the accelerometers back to back. Three different calibration constants were used. All tests were made with the exciter acceleration set at 10 G. Phase shift in the electronics was carefully checked. The transverse vibration of the bar was checked with a stroboscope and found to be insignificant. The signals showed no visible distortion.

All data were recorded when the phase angle between the two signals was 90° . The value of Q' was measured and the frequency was recorded. ξ' , $\tan \delta/2$, E^* , E_1 , E_2 and base stress were then computed using the computer program given in Appendix A. The experimental results are presented in Figures 11 and 12 and the computed results are presented in Table II.

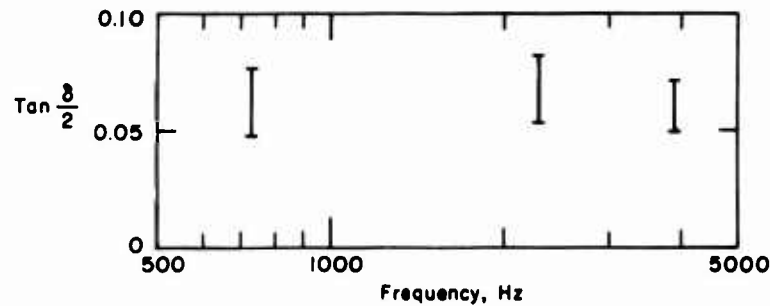


a. End mass accounted for.

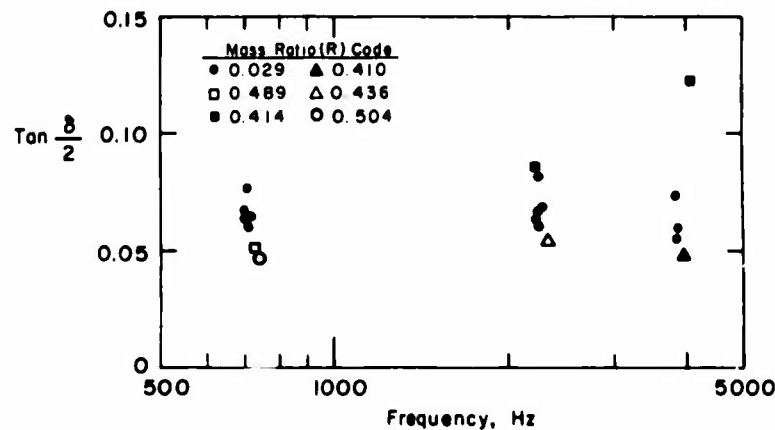


b. End mass neglected in theory.

Figure 11. Experimental results, E^* vs frequency.



a. End mass accounted for.



b. End mass neglected in theory.

Figure 12. Experimental results, $\tan \delta/2$ vs frequency.

Table II. Computed results using experimental data.*

Test no.	Mass ratio R	Bar length (in.)	Frequency f' (Hz)	Accel ratio Q'	Frequency ratio ξ	$\tan \delta/2$	E^* (psi)	E_1 (psi)	E_2 (psi)
1	0.029	10.02	704	8.21	1.53	0.0771	72160	71302	11097
2	.029	10.02	2236	2.53	4.58	.0811	80843	79780	13067
3	.029	10.02	3842	1.66	7.64	.0711	85858	84989	12182
35	.029	10.00	712	10.25	1.53	.0619	73517	72954	9076
36	.029	10.00	2228	3.40	4.58	.0610	79952	79357	9737
37	.029	10.00	3830	2.12	7.64	.0568	84994	84446	9632
38	.029	10.00	3830	2.18	7.64	.0553	84995	84475	9384
39	.029	10.00	2215	3.34	4.58	.0621	79022	78413	9791
40	.029	10.00	707	9.68	1.53	.0655	72487	71866	9471
41	.029	10.00	718	9.71	1.53	.0653	74760	74123	9739
42	.029	10.00	2226	3.09	4.58	.0670	79807	79092	10659
43	.029	10.00	3839	2.05	7.64	.0586	85393	84807	9985
44	.029	10.00	702	9.83	1.53	.0645	71466	70871	9197
45	.029	10.00	2249	3.06	4.58	.0676	81460	80716	10962
46	.029	10.00	3882	2.03	7.64	.0591	87316	86706	10304
59	.489	7.00	722	12.42	1.08	.0475	73470	73139	6963
61	.414	8.25	2215	2.43	3.72	.0530	81364	80908	8600
62	.414	8.25	4067	0.91	6.65	.0528	86103	85626	9047
79	.504	6.69	738	12.50	1.08	.0471	71259	70943	6696
85	.410	8.25	3991	0.99	6.65	.0489	82887	82491	8089
86	.436	7.75	2326	2.33	3.70	.0539	80051	79585	8616

* ξ , $\tan \delta/2$, E^* , E_1 , and E_2 were computed using the computer program of Appendix A.

Experimental results

The ranges of E^* and $\tan \delta/2$ which were computed from the experimental values of Q' and f' for various mass ratios are shown in the upper portion of Figures 11 and 12, respectively, at the frequencies corresponding to the first three modes of vibration. To illustrate the errors introduced in computing the complex modulus ignoring end-mass effect, the lower halves of these figures are plots of the same data calculated from theory neglecting end-mass effect. All data are taken from Table II and there are seven points at each frequency (some are superimposed).

It may be concluded that large errors are introduced in the computation of E^* if mass loading effects are neglected. For example, for R as low as 0.029, E^* will be about 6% low in the first three modes; for $R = 0.5$, E^* will be about 50% of its true value in the first mode. This is illustrated graphically in Figure 11.

The effect of mass loading on the computation of $\tan \delta/2$ is seen in Figure 12. The errors introduced using $R = 0$ theory are about 1% for $R = 0.029$ but become greater with increased mass ratio and mode number. For example, Young (1967) gives an error of 130.6% high for $\tan \delta/2$ for $R = 0.414$ in the third mode. The spread in the experimental data for $\tan \delta/2$ for constant values of R makes it difficult to interpret the data in these tests.

CONCLUSIONS AND SUMMARY

The theory given here, including end-mass effect, leads to more nearly correct results in computing the complex modulus from vibrating bar test data and should be adopted. For laboratories

using the 90° phase shift measurement technique, this report presents curves that allow direct use of experimental data to calculate the complex modulus. For experimental data that fall outside the range of these curves, a computer program is presented for the same purpose.

LITERATURE CITED

- Brown, G.W. and Selway, D.R. (1964) Frequency response of a photoviscoelastic material. *Experimental Mechanics*, vol. 4, p. 57-63.
- Kuo, S.S. (1965) *Numerical methods and computers*. Reading, Mass.: Addison Wesley.
- Lee, T.M. (1963) Method of determining properties of viscoelastic solids employing forced vibration. *Journal of Applied Physics*, vol. 34, p. 1524-1529.
- Scarborough, J.B. (1955) *Numerical mathematical analysis*. Baltimore: The Johns Hopkins Press, p. 203-204.
- Timoshenko, S. (1955) *Vibration problems in engineering*, 3rd Ed. New York: D. Van Nostrand, p. 312-313.
- Young, Wun-Chung (1967) Forced longitudinal vibration of a viscoelastic bar with end mass. University of New Hampshire, Master's Thesis.

APPENDIX A. TAN $\delta/2$ AND E^* FROM MEASURED Q' AND FREQUENCY

```

WRITE(3,21)
31 READ(1,1) A,B,RO,AL,LF,N,UO
1 FORMAT(3F10.7,F10.4,15.15,F10.7)
IF(N) 4,40,4
4 B1=1./B
C THE FOLLOWING 4 STATEMENTS ARE USED FOR CALCULATING THE
C FIRST TRIAL VALUE OF LOSS FACTOR, DEL/2.
XN=N
EPS=0.0001
PI=3.14159
X=PI*(2.*XN-1.)/2.
ASIN=ALOG((1.+SQRT(1.+B**2))/B)
Y=ASIN/X
GO TO (2,6,2,6,2,6),N
6 B1=-B1
C THE FOLLOWING 15 STATEMENTS ARE FOR THE ITERATIONS
2 SINH=(EXP(X*Y)-EXP(-X*Y))/2.
COSH=(EXP(X*Y)+EXP(-X*Y))/2.
F1=COSH*(COS(X)-A*X*SIN(X))+A*X*Y*COS(X)*SINH
F2=SINH*(SIN(X)+A*X*COS(X))+COSH*A*X*Y*SIN(X)-B1
F1XT2=COSH*(-(1.+A)*SIN(X)-A*X*(1.-Y*Y)*COS(X))
F2XT2=COSH*((1.+A)*Y*SIN(X)+2.*A*X*Y*COS(X))
F1X=SINH*((1.+A)*Y*COS(X)-2.*A*X*Y*SIN(X))+F1XT2
F2X=SINH*((1.+A)*COS(X)-A*X*(1.-Y*Y)*SIN(X))+F2XT2
F1Y=SINH*((1.+A)*X*COS(X)-A*X*X*SIN(X))+COSH*A*X*X*Y*COS(X)
F2Y=COSH*((1.+A)*X*SIN(X)+A*X*X*COS(X))+SINH*A*X*X*Y*SIN(X)
H=F1X*F2Y-F1Y*F2X
HX=F1*F2Y-F2*F1Y
HY=F2*F1X-F1*F2X
DELX=-HX/H
DELY=-HY/H
IF(ABS(DELY)-EPS) 5,5,10
5 IF(ABS(DELY)-EPS) 30,30,10
10 X=X+DELX
Y=Y+DELY
GO TO 2
30 DELTA=2.*ATAN(Y)
C=(2.*PI*LF*AL)/X
RO=(RO*0.07615)/(32.2*12.)
F=RO*(C*COS(DELTA/2.))**2
IF1=F*COS(DELTA)
IF2=F*SIN(DELTA)
C STRESS CALCULATION
COFF=UO*X*EAB/AL
AS=SIN(X)+A*X*COS(X)
BS=COS(X)-A*X*SIN(X)
CS=A*X*Y
REALL=BS*SINH+CS*COS(X)*COSH
AMIGG=AS*COSH+CS*SIN(X)*SINH
STRESS=COFF*SQRT((AMIGG*Y-REALL)**2+(REALL*Y+AMIGG)**2)
IC=C
IF=F
WRITE(3,22) A,B,LF,X,Y,IC,IF,IF1,IF2,STRESS,AL
GO TO 31
40 CALL EXIT

```

```

21 FORMAT(1H1,6X,1HR,8X,1HQ,6X,6HF(CPS),6X,6HXL/Z,6X,6HDEL/2,6X,
19HC(1N/SEC),5X,6HE(PSI),8X,2HE1,10X,2HE2,8X,6HSTR,5X,6X,
18HL OF BAR/)
22 FORMAT(F10.3,F8.2,2X,18,2X,F10.3,1X,F10.4,6X,17,5X,17,5X,17,4X,17,
14X,F10.6,5X,F5.2)
END

```

C TYPICAL INPUT

C	R	Q	SG	L	F	N	DISPL
0.0	8.97	0.911	13.9	02269	01	1.952E-06	
0.07153	8.97	0.911	13.9	02269	01	1.952E-06	
0.0	25.6	0.911	13.9	06639	02	0.875E-07	
0.07153	25.6	0.911	13.9	06639	02	0.875E-07	
0.0	17.6	0.911	13.9	10983	03	0.535E-07	
0.07153	17.6	0.911	13.9	10983	03	0.535E-07	

C TYPICAL OUTPUT

R	Q	F(CPS)	WL/C	DEL/2	C(1N/SEC)
0.0	8.97	2269	1.571	0.0708	126156
0.072	8.97	2269	1.466	0.0705	135140
0.0	25.60	6639	4.712	0.0083	123042
0.072	25.60	6639	4.407	0.0079	131567
0.0	17.60	10983	7.854	0.0072	122130
0.072	17.60	10983	7.369	0.0065	130168

E(PSI)	E1	E2	STRESS	L OF BAR
1349692	1336218	190230	2.691124	13.90
1548847	1533538	217226	2.898381	13.90
1290243	1290065	21383	0.980596	13.90
1475233	1475047	23413	1.099324	13.90
1271209	1271076	18381	0.677436	13.90
1444042	1443921	18663	0.815897	13.90

**APPENDIX B. STRESS, STRAIN AND DISPLACEMENT AS A FUNCTION
OF X AND R (TABLE I)**

```

      COMPLEX P,PL,C2,GAMA, XI ,EPS,SIGMA,DISPL,BIC,BC,YC,EPSI
100 READ(1,2) Y,UZ,R,AL,E,X,KOUNT
      2 FORMAT(3F10.8,F10.5,F10.0,F10.5,12)
      IF(KOUNT)5,7,5
      5 WRITE(3,1)
      Y=2.*ATAN(Y)
      A1=X
      B1=X*TAN(Y/2.)
      BIC=(0.0,1.0)*B1
      PL=A1-BIC
      P=PL/AL
      GAMA=R*PL
      C2=(CSIN(PL)+GAMA*CCOS(PL))/(CCOS(PL)-GAMA*CSIN(PL))
      ZN=0.0
11 A=ZN*X
      B=A*TAN(Y/2.)
      BC=(0.0,1.0)*B
      XI =A-BC
      EPS=UZ*P*(C2*CCOS(XI)-CSIN(XI))
      YC=(0.0,1.0)*Y
      EPSI=EPS*CEXP(YC)
      SIGMA=E*CEXP(YC)*EPS
      DISPL=UZ*(CCOS(XI)+C2*CSIN(XI)-1.)
      DISPLS=CABS(DISPL)
      DISPLR=REAL(DISPL)
      DISPLI=AIMAG(DISPL)
      IF(DISPLR) 15,16,15
16 DPHASE=0.0
      GO TO 25
15 DPHASE=ATAN(DISPLI/DISPLR)
25 SIGMAS=CABS(SIGMA)
      SIGMAR=REAL(SIGMA)
      SIGMAI=AIMAG(SIGMA)
      IF(SIGMAR) 17,18,17
17 SPHASE=ATAN(SIGMAI/SIGMAR)
18 EPSSE=CABS(EPS)
      EPSR=REAL(EPS)
      EPSI=AIMAG(EPS)
      IF(EPSR) 19,20,19
19 EPHASE=ATAN(EPSI/EPSR)
20 WRITE(3,3) DISPL,SIGMA,EPSI
      WRITE(3,21) DISPLS,SIGMAS,EPSSE
      WRITE(3,21) DPHASE,SPHASE,EPHASE
      ZN=ZN+0.25
      IF(ZN-1.20) 11,12,12
12 WRITE(3,6)
      GO TO 100
7 CALL EXIT
1 FORMAT(1H1,5X,12H)DISPLACEMENT,20X,6H)STRESS,23X,6H)STRAIN(
3 FORMAT(/2G12.4,5X,2G12.4,5X,2G12.4)
21 FORMAT(G12.4,12X,G12.4,12X,G12.4)
6 FORMAT(//)
4 FORMAT(15)
      END

```


APPENDIX C. Q VERSUS ξ FOR VARIOUS R AND TAN $\delta/2$ VALUES
(FIG. 2-4)

C	DATA FOR APPENDIX C	PROGRAM
1C=1		
ICC=90		
CALL PLOT(1C,3.0,5.0,5.0,0.5,0.0,2.0,0.0,4.0,0.3,0.0,1.0)		
CALL PLOT(99)		
WRITE(3,2)		
5 READ(1,6) A,X,TANY	3.0	0.06
IF(A=0.6) 8,7,7	3.0	0.10
8 SAM=-1.	3.0	0.20
DO 25 K=1,10	3.0	0.06
DO 10 I=1,80	3.0	0.10
X=X+0.0025	3.0	0.20
COSH=(EXP(X*TANY)+EXP(-X*TANY))/2.		
SINH=(EXP(X*TANY)-EXP(-X*TANY))/2.	5.8	0.06
F1=COSH*(COS(X)-A*X*SIN(X))+A*X*TANY*COS(X)*SINH	5.8	0.10
F2=SINH*(SIN(X)+A*X*COS(X))+A*X*TANY*SIN(X)*COSH	5.8	0.20
Z=SQRT(F1**2+F2**2)	5.8	0.06
Z=1./Z	5.8	0.06
IF(F1*SAM) 12,12,14	5.8	0.10
12 CALL PLOT(0,X,Z)	5.8	0.20
SAM=F1		
GO TO 10		
14 CALL PLOT(ICC,X,Z)		
10 CONTINUE		
25 CONTINUE		
CALL PLOT(99)		
GO TO 5		
7 CALL PLOT(7)		
CALL PLOT(1C,5.8,8.2,6.0,0.0,2.0,0.0,3.0,0.6,0.1,0)		
CALL PLOT(99)		
15 READ(1,6) A,X,TANY		
IF(A=0.6) 18,17,17		
18 SAM=1.		
DO 125 K=1,12		
DO 110 I=1,80		
X=X+0.0025		
COSH=(EXP(X*TANY)+EXP(-X*TANY))/2.		
SINH=(EXP(X*TANY)-EXP(-X*TANY))/2.		
F1=COSH*(COS(X)-A*X*SIN(X))+A*X*TANY*COS(X)*SINH		
F2=SINH*(SIN(X)+A*X*COS(X))+A*X*TANY*SIN(X)*COSH		
Z=SQRT(F1**2+F2**2)		
Z=1./Z		
IF(F1*SAM) 112,112,114		
112 CALL PLOT(0,X,Z)		
SAM=F1		
GO TO 110		
114 CALL PLOT(ICC,X,7)		
110 CONTINUE		
125 CONTINUE		
CALL PLOT(99)		
GO TO 15		
17 CALL PLOT(100)		
CALL EXIT		
2 FORMAT(1H1,5X,1HP,6X,8HTANDEL/2,5X,1HX,9X,1H0/)		
6 FORMAT(4F10.5)		
END		

APPENDIX D. ξ VERSUS R FOR VARIOUS VALUES OF TAN $\delta/2$ (FIG. 5)

C

```

      IC=1
      ICC=90
      DO 11 I=1,2
      READ(1,22)
11  WRITE(3,22)
22  FORMAT(1X,79H
      1
      EPS=0.001
      CALL PLOT(1C,0.0,0.0,6.6,0.0,0.1,0.0,10.0,10.0,1.0)
      CALL PLOT(99)
30  READ(1,3) X11,X22,Y,N
      IF(X11) 6,7,6
      6  WRITE(3,4) N
      R=-0.00125
      DO 25 K=1,6
      DO 10 I=1,80
      X1=X11
      X2=X22
      R=R+0.00125
      P1=3.14159
      COT1=COS(X1)/SIN(X1)
      COT2=COS(X2)/SIN(X2)
      FX1=COT1-R*X1+R*X1*Y*COT1*TANH(X1*Y)
      FX2=COT2-R*X2+R*X2*Y*COT2*TANH(X2*Y)
70  X=(X1+X2)/2.
      CX=COS(X)/SIN(X)
      FX=COTX-R*X+R*X*Y*COTX*TANH(X*Y)
      IF(ABS(FX)-EPS) 15,15,60
60  IF(FX*FX1) 50,15,80
50  X2=X
      FX2=FX
      GO TO 70
80  X1=X
      FX1=FX
      GO TO 70
15  CALL PLOT(ICC,R,X)
10  CONTINUE
      WRITE(3,1) Y,R,X
25  CONTINUE
      CALL PLOT(99)
      GO TO 30
      7  CALL PLOT(100)
      CALL EXIT
      1  FORMAT(5F10.5)
      3  FORMAT(3F10.5,12)
      4  FORMAT(//5X,4HN = .12//)
      END

```

C	DATA FOR APPENDIX D			PROGRAM
	Y	R	X	
0.8	1.8	0.0	01	
0.8	1.8	0.1	01	
0.8	1.8	0.2	01	
3.4	5.0	0.0	02	
3.4	5.0	0.1	02	
3.4	5.0	0.2	02	
6.5	9.0	0.0	03	
6.5	9.0	0.1	03	
6.5	9.0	0.2	03	
0.0				

DOCUMENT CONTROL DATA - R & D		
(Security classification of title, body of abstract and indexing annotation must be entered when the overall report is classified)		
1. ORIGINATING ACTIVITY (Corporate author) U. S. Army Cold Regions Research and Engineering Laboratory Hanover, New Hampshire 03755		2a. REPORT SECURITY CLASSIFICATION Unclassified
		2b. GROUP
3. REPORT TITLE LONGITUDINAL FORCED VIBRATION OF VISCOELASTIC BARS WITH END MASS		
4. DESCRIPTIVE NOTES (Type of report and inclusive dates)		
5. AUTHOR(S) (First name, middle initial, last name) D. M. Norris, Jr. and Wun-Chung Young		
6. REPORT DATE April 1970	7a. TOTAL NO. OF PAGES 29	7b. NO. OF REFS 6
8a. CONTRACT OR GRANT NO. DA-AMC-27-021-67-G21	9a. ORIGINATOR'S REPORT NUMBER(S) Special Report 135	
b. PROJECT NO.		
c.	9b. OTHER REPORT NO(S) (Any other numbers that may be assigned this report)	
d.		
10. DISTRIBUTION STATEMENT This document has been approved for public release and sale; its distribution is unlimited.		
11. SUPPLEMENTARY NOTES		12. SPONSORING MILITARY ACTIVITY U. S. Army Cold Regions Research and Engineering Laboratory Hanover, New Hampshire 03755
13. ABSTRACT A simple method is presented to measure the complex modulus of suitably rigid linear viscoelastic materials over the audiofrequency spectrum. The case is considered where one end of a rod of the material is driven harmonically and the complex displacement ratio is measured. The effect of a rigid end mass on the free end is accounted for. It is shown that, at specific frequencies near resonance, it is easy to obtain modulus data with standard equipment usually found in the vibration laboratory. An experimental program is described.		
14. Key Words Audiofrequencies Shear modulus Viscoelastic materials		